

Abundance ratios of red giants in low mass ultra faint dwarf spheroidal galaxies

P. François^{1,2}, L. Monaco³, P. Bonifacio¹, C. Moni Bidin⁴, D. Geisler⁵, and L. Sbordone^{6*}

¹ GEPI, Observatoire de Paris, PSL Research University, CNRS, Univ Paris Diderot, Sorbonne Paris Cit, 61 Avenue de l'Observatoire, 75014 Paris, France

e-mail: patrick.francois@obspm.fr

² Université de Picardie Jules Verne, 33 rue St Leu, Amiens, France

³ Departamento de Ciencias Físicas, Universidad Andres Bello, Republica 220, Santiago, Chile

⁴ Instituto de Astronomía, Universidad Católica del Norte, Av. Angamos 0610, Antofagasta, Chile

⁵ Department of Astronomy Faculty of Physical and Mathematical Sciences, University of Concepción, Chile

⁶ Millennium Institute of Astrophysics, Pontificia Universidad Católica de Chile, Vicuña Mackenna 4860, Macul Santiago, Chile

Received ; accepted

ABSTRACT

Context. Low mass dwarf spheroidal galaxies are key objects for our understanding of the chemical evolution of the pristine Universe and the Local Group of galaxies. Abundance ratios in stars of these objects can be used to better understand their star formation and chemical evolution.

Aims. We report on the analysis of a sample of 11 stars belonging to 5 different ultra faint dwarf spheroidal galaxies (UfDSph) based on X-Shooter spectra obtained at the VLT.

Methods. Medium resolution spectra have been used to determine the detailed chemical composition of their atmosphere. We performed a standard 1D LTE analysis to compute the abundances.

Results. Considering all the stars as representative of the same population of low mass galaxies, we found that the $[\alpha/\text{Fe}]$ ratios vs $[\text{Fe}/\text{H}]$ decreases as the metallicity of the star increases in a way similar to what is found for the population of stars belonging to dwarf spheroidal galaxies. The main difference is that the solar $[\alpha/\text{Fe}]$ is reached at a much lower metallicity for the UfDSph than the dwarf spheroidal galaxies.

We report for the first time the abundance of strontium in CVnI. The star we analyzed in this galaxy has a very high $[\text{Sr}/\text{Fe}]$ and a very low upper limit of barium which makes it a star with an exceptionally high $[\text{Sr}/\text{Ba}]$ ratio.

Our results seem to indicate that the galaxies which have produced the bulk of their stars before the reionization (fossil galaxies) have lower $[X/\text{Fe}]$ ratios at a given metallicity than the galaxies that have experienced a discontinuity in their star formation rate (quenching).

Key words. Galaxies - Stars - abundances

1. Introduction

A cold dark matter cosmological models are in agreement with many observable phenomena, but some discrepancies are found on small scales. In particular, this model predicts too many dark-matter sub-halos (a factor of 50) that the number of observed dwarf galaxies (Moore et al. , 1999). A solution to this problem was put forward by Bullock et al. (2000) who suggested that gas accretion in low-mass halos could be suppressed by the photo-ionization mechanism during the reionization of the Universe. The observed dwarf satellites correspond to the small fraction of halos that accreted enough amounts of gas before reionization. Based on this hypothesis, Ricotti & Gnedin (2005) proposed that dwarf galaxies could be classified in three different classes depending on the occurrence of their star formation relatively to the reionization event. Dwarf galaxies that formed most of their stars prior to the reionization are classified as "true fossils". From this classification, it appears that some stars we observe today in the so-called ultra faint dwarf spheroidal galaxies (UfDSph, Belokurov et al. (2007)) could be "survivors" of the reionization period. Brown et al. (2014) analyzed the star formation history of six UfDSphs (Bootes I, Canes Venatici II, Coma Berenices, Hercules, Leo IV and Ursa Major I). They concluded that five out of them are best fit by a star formation history where at least 75 % of the stars formed by $z \simeq 10$ and 100 % of the stars formed by $z \simeq 3$ i.e. 11.6 Gyrs ago, supporting the hypothesis of a quenching of the star formation by a global external influence such as reionization. The detailed chemical composition of stars in ultra-faint dwarf spheroidal galaxies is therefore an important tool to probe the early evolution of the local group. This paper reports on the detailed abundance determination of stars belonging to the UfDSphs Bootes II, Canes Venatici I, Canes Venatici II, Hercules and Leo IV. Among these five galaxies, two (Leo IV and Hercules) are consistent with the hypothesis that the bulk of their stars were formed before reionization (Weisz et al. , 2014). However, their conclusion has been challenged (Brown et al. , 2014) . Three of our galaxies were analyzed by Brown et al. (2014). Using deep and high S/N ACS imaging over a wide field, they found that these galaxies (and three others, among them BooI) were consistent with the hypothesis that reionization ended star formation in all of them.

Webster et al. (2015) have modeled the chemical evolution of the six UfDsph galaxies studied by Brown et al. (2014) , among them Boo I, CVnI, Hercules and LeoIV). They showed that two single-age bursts cannot explain the observed $[\alpha/\text{Fe}]$ versus $[\text{Fe}/\text{H}]$ distribution in these galaxies. They suggested an alternative scenario in which star formation is continuous except for short interruptions. From their table 1, Hercules and LeoIV have the same likelihood to have quenched or non-quenched star formation history. If we take into account of the studies made by Weisz et al. (2014) and Brown et al. (2014), these two galaxies can be considered as "fossil" galaxies. On the other hand, Boo I and CVnII have a higher likelihood to have an extended star formation history. Based on the results from Webster et al. (2015) we classify Her and LeoIV as "fossil galaxies" and CVnII, BooI and CVnI as galaxies with extended star formation history.

Before going into the details of our analysis, we would like to remind the most important characteristics of each galaxy for which we obtained mid-resolution spectra with the ESO-VLT and the X-Shooter spectrograph.

* Based on observations made with ESO Telescopes at the La Silla Paranal Observatory under programme ID 085.B-0367(A)

1.1. *Bootes II*

The discovery of Bootes II was reported by Walsh et al. (2007) as an over density on the Sloan Digital Sky Data Release 5 (hereafter SDSS DR5) distribution. From isochrone fitting techniques and accurate color-magnitude diagram, they described Bootes II as an old (12 Gr), metal-poor ($[\text{Fe}/\text{H}] \simeq -2.00$ dex) galaxy with a distance estimated at 60 kpc. MMT/Megacam imaging in Sloan g and r (Walsch et al. , 2008) led a to a revised distance of 42 ± 2 kpc. From follow-up spectroscopy of five member stars, Koch et al. (2008) found a mean metallicity of $[\text{Fe}/\text{H}] = -1.79 \pm 0.05$ dex. This determination relies on an old calibration of the Ca triplet which was revised later on. Koch & Rich (2014) made a detailed chemical analysis of the brightest confirmed member star in Boo II using Keck/Hires and derived a very low metallicity of $[\text{Fe}/\text{H}] = -2.93$ dex using an updated Ca triplet calibration. They also found a high $[\alpha/\text{Fe}]$ ratio compatible with the α -enhanced plateau value of the galactic halo.

1.2. *Canes Venatici I*

Canes Venatici I was discovered in 2006 by Zucker et al. (2006) as a stellar over density in the north Galactic cap using the Sloan Digital Sky Survey Data Release 5. From the tip of the red giant branch, they concluded that the Galaxy was at a distance of $\simeq 220$ kpc. The first deep color-magnitude diagrams of the Canes Venatici I (CVn I) dwarf galaxy were provided by Martin et al. (2008) from observations with the wide-field Large Binocular Camera on the Large Binocular Telescope. Interestingly, their analysis revealed a dichotomy in the stellar populations of CVn I which harbors an old (≥ 10 Gyrs), metal-poor ($[\text{Fe}/\text{H}] \simeq -2.0$), and spatially extended population along with a much younger, more metal-rich and spatially more concentrated population. However, the claim of a young population in Canes Venatici I has not been supported by more recent studies (Ural et al. , 2010; Okamoto et al. , 2012) . Martin et al. (2008) derived a distance modulus of $(m - M)_0 = 21.69 \pm 0.10$ or $D = 218 \pm 10$ kpc . Okamoto et al. (2012) confirmed the distance modulus using deep images taken with the Subaru/Suprime-Cam imager obtaining a distance modulus of $(m - M)_0 = 21.68 \pm 0.08$ (216 ± 8 kpc) . Kirby et al. (2010) determine the abundances of Fe and several α elements in a sample of 171 stars using medium resolution spectra ($R \sim 7000$) obtained with Keck/DEIMOS and found metallicities ranging from -1.0 dex to -3.3 dex. No high resolution spectroscopy has been performed so far.

1.3. *Canes Venatici II*

The UfDSph Canes Venatici II is one of the four UfDSph discovered by Belokurov et al. (2007) in the Sloan digital Sky Survey. Follow-up spectroscopic observations were performed in 2008 by Kirby et al. (2008) who analyzed 16 stars. They used DEIMOS on the Keck II telescope to obtain spectra at $R \simeq 6000$ over a spectra range of roughly 6500-9000 Å. They derived a mean metallicity of $[\text{Fe}/\text{H}] = -2.19 \pm 0.05$ dex with a dispersion of 0.58 dex. Vargas et al. (2013) computed the $[\alpha/\text{Fe}]$ ratios in 8 stars of this galaxy and found an increase of the $[\alpha/\text{Fe}]$ as metallicity decreases with a solar ratio at $[\text{Fe}/\text{H}] \simeq -1.30$ dex to reach on average an $[\alpha/\text{Fe}] \simeq 0.5$ dex at $[\text{Fe}/\text{H}] \simeq -2.50$ dex. The distribution of $[\text{Ca}/\text{Fe}]$ and $[\text{Ti}/\text{Fe}]$ abundance ratios tends to point towards the presence

of a significant scatter at low $[\text{Fe}/\text{H}]$. The metallicity was later revised by Vargas et al. (2013) who found $[\text{Fe}/\text{H}] = -2.18 \pm 0.06$ dex.

1.4. *Hercules*

Hercules is a dwarf spheroidal satellite of the Milky Way, found at a distance of 138 kpc.

This UfDSph has been discovered by Belokurov et al. (2007). Coleman et al. (2007) performed deep wide-field photometry in B, V and r of this galaxy using the Large Binocular Telescope down to 1.5 mag below the main sequence turn-off and found that the Hercules dwarf is highly elongated suggesting tidal disruption as a likely cause. Simon et al. (2007) obtained a first estimate of the metallicity using Keck-DEIMOS spectroscopy of 30 stars finding $[\text{Fe}/\text{H}] \simeq -2.27$ with a dispersion of 0.31 dex. Koch et al. (2008) analyzed 2 red giants and derived a metallicity of $[\text{Fe}/\text{H}] \simeq -2.00$ dex with strong enhancements in Mg and O and a high deficiency in the neutron capture elements. Later, Adén et al. (2009) analyzed 11 stars in Hercules and obtained a metallicity spread ranging from $[\text{Fe}/\text{H}] = -2.03$ to -3.17 dex. They also found that the red giant branch stars are more metal-poor than previously estimated by photometry. A comparison of their spectroscopic stellar parameters with isochrones indicates that the giants in Hercules are older than 10 Gyrs. Koch et al. (2013) analyzed a new sample of four red giants and confirmed the high level of depletion of the neutron capture elements and suggested that the chemical evolution of Her was dominated by very massive stars. Deep g,i-band DECam stellar photometry of the Hercules Milky Way satellite galaxy, and its surrounding field, out to a radial distance of 5.4 times the tidal radius was done by Roderick et al. (2015). They identified nine extended stellar substructures associated with the dwarf, preferentially distributed along the major axis of the galaxy demonstrating that Hercules is a strongly tidally disrupted system.

1.5. *Leo IV*

The dwarf galaxy Leo IV was discovered by Belokurov et al. (2007) along with Coma Berenices, Canes Venatici II and Hercules. Simon et al. (2007) obtained Keck/DEIMOS spectra of a sample of stars belonging to this galaxy and derived a metallicity of $[\text{Fe}/\text{H}] = -2.31 \pm 0.10$ dex. Adopting a reddening $E(B - V) = 0.04 \pm 0.01$ mag and a metallicity of $[\text{Fe}/\text{H}] = -2.31 \pm 0.10$ dex. Moretti et al. (2009) derived a distance of 154 ± 5 kpc. The first determination of the chemical composition of stars in Leo IV was done by Simon et al. (2010). They obtained high resolution Magellan/MIKE spectra of the brightest star in Leo IV and measured an iron abundance $[\text{Fe}/\text{H}] = -3.2$ dex with an α element enhancement similar to what is found in the milky way halo. Interestingly, this star is among the most metal poor stars found in UfDSphs. Okamoto et al. (2012) estimated the average age of the stellar population to be 13.7 Gyrs by overlaying Padova isochrones. We present in this paper, the determination of the detailed chemical composition of two stars belonging to LeoIV. Vargas et al. (2013) revised the metallicity and found $[\text{Fe}/\text{H}] = -2.89 \pm 0.11$ dex .

2. Observations

The aim of these observations was the study of the metal-poor population of stars belonging to UfDSphs. Therefore the sample is biased towards the brightest targets among the metal poor sam-

Table 1. Target coordinates, Signal to noise ratios and radial velocities

Galaxy	Object	Other ID	RA	DEC	SNR at 500 nm	Vr km s ⁻¹
Boo II	SDSS J135801.42+125105.0	Boo II – 7	13h58m01.0s	12d51m04.7s	55	-138
Boo II	SDSS J135751.18+125136.9	Boo II – 15	13h57m51.2s	12d51m36.6s	60	-119
Leo IV	SDSS J113255.99-003027.8	Leo IV – S1	11h32m56.0s	-00d30m27.8s	35	126
Leo IV	SDSS J113258.70-003449.9		11h32m58.7s	-00d34m50.0s	50	129
CVn II	SDSS J125713.63+341846.9		12h57m13.6s	+34d18m46.9s	25	135
CVn I	SDSS J132755.65+333324.5		13h27m55.7s	+33d33m24.5s	30	21
CVn I	SDSS J132844.25+333411.8		13h28m44.3s	+33d34m11.8s	35	21
Her	SDSS J163044.49+124947.8		16h30m44.5s	+12d49m47.9s	45	35
Her	SDSS J163059.32+124725.6		16h30m59.3s	+12d47m25.6s	50	36
Her	SDSS J163114.06+124526.6		16h31m14.1s	+12d45m26.6s	70	49
Her	SDSS J163104.50+124614.4		16h31m04.5s	+12d46m14.5s	35	40

ple of these galaxies. Target stars were selected from among the most metal-poor radial velocity member stars with $V < 20.0$ in each galaxy, and were extracted from published low-resolution studies (Kirby et al. , 2008; Koch et al. , 2009). All of the targets have putative metallicities $[\text{Fe}/\text{H}] < -2.0$ dex , 9 out of 11 having $[\text{Fe}/\text{H}]_j < -2.6$, i.e. more metal-poor than any Galactic globular cluster. From their CaT index, seven stars have $[\text{Fe}/\text{H}] < -3.0$ dex and are, therefore, extremely metal-poor.

The observations were performed in service mode with the ESO-Kueyen telescope (VLT UT2) and the high-efficiency spectrograph X-Shooter (D’Odorico et al. , 2006; Vernet et al. , 2011). The list of targets is given in table 1.

The observations have been performed in staring mode with 1x1 binning and the integral field unit (IFU). We used the IFU as a slicer with three 0.6'' slices. This corresponds to a resolving power of $R = 7900$ in the ultra-violet arm (UVB) and $R = 12600$ in the visible arm (VIS). The stellar light is divided in three arms by X-Shooter; we analyzed here only the UVB and VIS spectra. The stars we observed are very faint and have most of their flux in the blue part of the spectrum, so that the signal-to-noise ratio (S/N) of the infra-red spectra is too low to allow a reliable chemical abundance analysis. Moreover, the sky contamination in staring mode affects strongly the stellar spectrum. The spectra were reduced using the X-Shooter pipeline (Goldoni et al. , 2006), which performs the bias and background subtraction, cosmic-ray-hit removal (Van Dokkum , 2001), sky subtraction (Kelson , 2003), flat-fielding, order extraction, and merging. However, the spectra were not reduced using the IFU pipeline recipes. Each of the three slices of the spectra were instead reduced separately in slit mode with a manual localization of the source and the sky. This method allowed us to perform the best possible extraction of the spectra, leading to an efficient cleaning of the remaining cosmic ray hits, but also to a noticeable improvement in the S/N, thanks to the optimal extraction pipeline routine of X-Shooter. Using the IFU can cause some problems with the sky subtraction because there is only $\pm 1''$ on both sides of the object. In the case of a large gradient in the spectral flux (caused by emission lines), the modeling of the sky-background signal can be of poor quality owing to the small number of points used in the modeling. As we made our analysis only in the UVB and VIS spectra of X-Shooter, only few lines are affected by this problem.

Table 2. Log of the observations. All the exposures are of 2950 seconds.

OBJECT	TIMESTAMP
SDSS J113258.70-003449.9 / Leo IV	2011-02-07T07:11:20.295
SDSS J113258.70-003449.9 / Leo IV	2011-02-07T08:17:40.984
SDSS J125713.63+341846.9 / CVn II	2010-04-02T06:36:39.302
SDSS J125713.63+341846.9 / CVn II	2011-04-09T04:33:13.527
SDSS J125713.63+341846.9 / CVn II	2011-04-09T05:43:44.497
SDSS J132844.25+333411.8 / CVn I	2011-05-04T13:01:06
SDSS J132844.25+333411.8 / CVn I	2011-04-27T04:23:11.240
SDSS J113258.70-003449.9 / Leo IV	2010-05-10T03:02:20.251
SDSS J113258.70-003449.9 / Leo IV	2010-05-10T04:10:07.978
SDSS J135751.18+125136.9 / Boo II – 15	2010-05-12T02:26:01.360
SDSS J135751.18+125136.9 / Boo II – 15	2010-05-12T03:21:50.970
SDSS J113255.99-003027.8 / Leo IV – S1	2010-06-10T02:12:37.200
SDSS J135801.42+125105.0 / Boo II – 7	2010-06-10T03:35:48.990
SDSS J163044.49+124947.8 / Her	2011-05-13T14:39:48
SDSS J132755.65+333324.5 / CVn I	2010-06-12T02:13:14.498
SDSS J163044.49+124947.8 / Her	2010-06-12T05:06:48.771
SDSS J163044.49+124947.8 / Her	2010-07-09T05:11:07.059
SDSS J163059.32+124725.6 / Her	2010-07-10T04:11:23.800
SDSS J163104.50+124614.4 / Her	2010-07-13T04:04:06.392
SDSS J135801.42+125105.0 / Boo II – 7	2010-08-03T00:28:32.920
SDSS J135801.42+125105.0 / Boo II – 7	2010-08-04T00:45:15.158
SDSS J163114.06+124526.6 / Her	2010-08-03T02:43:58.485
SDSS J135801.42+125105.0 / Boo II – 7	2010-08-05T00:27:02.020
SDSS J163104.50+124614.4 / Her	2010-08-05T01:34:40.556
SDSS J163104.50+124614.4 / Her	2010-08-09T03:03:43.065
SDSS J163104.50+124614.4 / Her	2010-08-10T01:43:39.930

We used the strong lines of magnesium to determine the radial velocities of the stars using the cross-correlation of the synthetic spectrum with the observed spectrum. Heliocentric corrections have been also applied. The radial velocities of the stars are reported in table 1. Typical errors of 5 km s^{-1} have been estimated by computing the dispersion of the measurements of the radial velocities on the individual spectra before combining them for the abundance determination. The results are in good agreement with the systemic radial velocities of the parent galaxies.

3. Analysis

The effective temperature was derived from the $(g-i)$ colors (Koch et al. , 2009) for the two Bootes stars and the V and I_C colors taken from Kirby et al. (2008) for the remaining stars. $(g-i)$ have been transformed into $(V-I_C)$ using the relation given by Jordi et al. (2006). The reddening correction is from Schlegel et al. (1998). We adopted the calibration of Ramírez & Meléndez (2005), use of the Alonso et al. (1999) calibration would result in temperatures that are 100 K to 150 K hotter. Note that all the published color calibrations are ill defined for very metal-poor giants, due to a scarcity of calibrators. The Ramírez & Meléndez (2005) sample of calibrators has more metal-poor giants

Table 3. Stellar parameters

Star	T_{eff} K	$\log g$ dex	ξ km s ⁻¹	[Fe/H] dex
SDSS J163044.49+124947.8 / Her	4700	1.40	2.1	-2.54
SDSS J163059.32+124725.6 / Her	4600	1.20	2.2	-2.85
SDSS J163104.50+124614.4 / Her	4870	1.70	2.2	-2.55
SDSS J163114.06+124526.6 / Her	4750	1.40	2.0	-2.30
SDSS J113255.99-003027.8 / Leo IV – S1	4500	1.10	2.5	-2.90
SDSS J113258.70-003449.9 / Leo IV	4800	1.50	2.4	-2.20
SDSS J125713.63+341846.9 / CVn II	4590	1.20	2.0	-2.60
SDSS J135801.42+125105.0 / Boo II – 7	4910	2.50	2.0	-3.10
SDSS J135751.18+125136.9 / Boo II – 15	4980	2.60	2.3	-3.00
SDSS J132844.25+333411.8 / CVn I	4450	0.81	2.0	-2.50
SDSS J132755.65+333324.5 / CVn I	4350	0.72	2.3	-2.20

than the Alonso et al. (1999) sample, hence our choice. The surface gravities have been obtained from the photometry and calculated using the standard relation between $\log g$, mass, T_{eff} and M_{bol} relative to the Sun, assuming the solar values $T_{\text{eff},\odot} = 5790$ K, $\log g = 4.44$ and $M_{\text{bol}} = 4.72$. We assumed also $0.8 M_{\odot}$ for the mass of the giant stars which have been observed. Distance moduli have been taken from Walsch et al. (2008) for BooII, from Kuehn et al. (2008) for CVnI, from Greco et al. (2008) for CVnII, from Musella et al. (2012) for Her and from Moretti et al. (2009) for LeoIV.

We carried out a classical 1D LTE analysis using OSMARCS model atmospheres (Gustafsson et al. , 1975; Plez et al. , 1992; Edvardsson et al. , 1993; Asplund et al. , 1997; Gustafsson et al. , 2003). The abundances used in the model atmospheres were solar-scaled with respect to the Grevesse & Sauval (2000) solar abundances, except for the α elements that are enhanced by 0.4 dex. We corrected the resulting abundances by taking into account the difference between Grevesse & Sauval (2000) and Caffau et al. (2011b), Lodders et al. (2009) solar abundances.

The abundance analysis was performed using the LTE spectral line analysis code turbospectrum (Alvarez & Plez 1998; Plez 2012), that treats scattering in detail. The carbon abundance was determined by fitting the CH band near at 430 nm (G band). The molecular data corresponding to the CH band are described in Hill et al. (2002) and Plez et al. (2008).

Two stars (HD 165195 and HE1249-3121) with published detailed abundances (Gratton et al. , 1994; Allen et al. , 2012) obtained using high resolution spectra have been used to check the validity of our abundance determinations. For these two stars, we retrieved X-shooter spectra and recomputed the abundances of the elements measured in our sample of UDSph galaxies stars. Our results are in agreement within 0.1 dex with the published abundances.

The adopted stellar parameters can be found in Table 3.

We measured the equivalent widths for a list of Fe I lines given in Table 4. With the assumed stellar parameters, we first checked the micro turbulent velocity using the method of the curves of growth (see for example Lemasle et al. (2008))

We checked the excitation temperature and refined the determination of the micro turbulent velocity parameters using the standard trends abundance vs excitation temperature and abundance vs

Table 4. List of lines used for the analysis. Hfs data for barium are from McWilliam & Preston (1995).

Wavelength	Ion	χ_{exc}	log gf
5889.950	Na I	0.00	0.11
5895.924	Na I	0.00	-0.19
4351.921	Mg I	4.34	-0.53
4571.102	Mg I	0.00	-5.39
5172.698	Mg I	2.71	-0.38
5183.619	Mg I	2.72	-0.16
5528.418	Mg I	4.34	-0.34
3944.016	Al I	0.00	-0.64
4226.740	Ca I	0.00	0.24
4283.014	Ca I	1.89	-0.22
6122.226	Ca I	1.89	-0.32
6162.173	Ca I	1.90	-0.09
4318.659	Ca I	1.90	-0.21
4030.763	Mn I	0.00	-0.48
4033.072	Mn I	0.00	-0.62
3920.269	Fe I	0.12	-1.75
3922.923	Fe I	0.05	-1.65
4045.825	Fe I	1.48	0.28
4063.605	Fe I	1.56	0.07
4071.749	Fe I	1.61	-0.02
4143.878	Fe I	1.56	-0.46
4181.764	Fe I	2.83	-0.18
4191.437	Fe I	2.47	-0.73
4202.040	Fe I	1.48	-0.70
4260.486	Fe I	2.40	-0.02
4282.412	Fe I	2.17	-0.82
4307.912	Fe I	1.56	-0.07
4383.557	Fe I	1.48	0.20
4404.761	Fe I	1.56	-0.14
4415.135	Fe I	1.61	-0.61
4427.317	Fe I	0.05	-2.92
4459.100	Fe I	2.18	-1.28
4461.660	Fe I	0.09	-3.20
4489.748	Fe I	0.12	-3.97
4494.573	Fe I	2.20	-1.14
4531.158	Fe I	1.48	-2.15
4920.514	Fe I	2.83	0.07
5083.345	Fe I	0.96	-2.96
5194.949	Fe I	1.56	-2.09
5371.501	Fe I	0.96	-1.65
5405.785	Fe I	0.99	-1.84
5429.706	Fe I	0.96	-1.88
5446.924	Fe I	0.99	-1.91
5455.624	Fe I	1.01	-2.09
g 6136.615	Fe I	2.45	-1.40
6191.571	Fe I	2.43	-1.42
4118.782	Co I	1.05	-0.49
4121.325	Co I	0.92	-0.32
5476.921	Ni I	1.83	0.89

Table 5. Error Budget

Element	ΔT_{eff} 100 K	$\Delta \log g$ 0.3 dex	$\Delta \xi$ 0.3 km s ⁻¹
Mg	0.12	-0.05	-0.12
Al	0.12	-0.10	-0.10
ScII	0.07	+0.05	-0.11
Ti	0.13	-0.04	-0.11
Mn	0.15	-0.06	-0.14
FeI	0.15	-0.06	-0.12
Ni	0.15	-0.04	-0.15
BaII	0.10	+0.09	-0.11
SrII	0.12	+0.10	-0.12

equivalent width. The iron excitation is satisfied for our adopted temperatures. It is standard practice to determine the gravity by imposing ionization balance on the Fe I and Fe II lines. Unfortunately, with the relatively low S/N and moderate resolution of our spectra, very few Fe II lines were detectable, and they are all either weak features and/or in low S/N regions of the spectrum. We therefore did not take into account these Fe II lines and determined the gravity from the photometry, as explained above.

For all the lines belonging to the elements other than Fe, we used the spectrum synthesis to determine the abundances.

4. Error budget

Table 5 lists an estimate of the errors due to typical uncertainties in the stellar parameters. These errors were estimated by varying T_{eff} , $\log g$ and ξ in the model atmosphere of SDSS J163114.06+124526.6 by the amounts indicated in the table. As the stars have similar stellar parameters, the other stars yield similar results. The total error is estimated by adding the quadratic sum of the the uncertainties in the stellar parameters and the error in the fitting procedure of the synthetic spectrum and the observed spectrum (the main source of error comes the incertitude in the placement of the continuum level).

5. Results and discussion

The resulting abundances can be found in Table 6. Fig 1 presents the [Mg/Fe] and [Ca/Fe] ratios found for our sample together with literature data for Milky Way field stars and stars in Dwarf Spheroidal galaxies. The majority of the stars shows a high [Mg/Fe] ratio comparable to what is found in the halo stars. The [Ca/Fe] ranges from $\simeq -0.05$ dex for a star in CVn I stars to $\simeq +0.65$ dex for BooII stars. This range is in agreement with the spread found for DSph stars, in the metallicity range -2.00 to -3.00 dex. It is interesting to note that the [Mg/Fe] and [Ca/Fe] ratios reach a solar value at a metallicity lower than the Milky Way field stars (where it is reached at $[\text{Fe}/\text{H}] \simeq 0.0$ dex) and than the dwarf galaxy stars for which the solar ratio is reached at metallicity around -2.00 to -1.50 dex in agreement with models of galactic chemical evolution (Vincenzo et al. , 2014).

Table 6. Detailed abundances : $[X/Fe]$ for all the elements except Fe for which $[Fe/H]$ is given.

Star	C	Na	Mg	Al	Ca	Mn
SDSS J163044.49+124947.8 / Her	—	0.01	0.23	—	-0.01	—
SDSS J163059.32+124725.6 / Her	—	0.02	0.34	0.15	0.29	—
SDSS J163104.50+124614.4 / Her	-0.34	0.00	0.29	0.23	0.25	—
SDSS J163114.06+124526.6 / Her	—	-0.15	-0.06	0.18	0.05	—
SDSS J113255.99-003027.8 / Leo IV – S1	—	0.10	0.44	—	—	—
SDSS J113258.70-003449.9 / Leo IV	—	0.05	-0.06	0.08	0.05	—
SDSS J125713.63+341846.9 / CVn II	—	-0.05	0.16	—	—	—
SDSS J135801.42+125105.0 / Boo II – 7	-0.24	—	0.29	0.28	0.25	0.04
SDSS J135751.18+125136.9 / Boo II – 15	-0.10	0.50	0.44	0.28	0.58	0.44
SDSS J132844.25+333411.8 / CVn I	—	—	0.46	—	0.29	—
SDSS J132755.65+333324.5 / CVn I	—	—	0.04	—	-0.10	—
	Ti	Fe	Co	Ni	Sr	Ba
SDSS J163044.49+124947.8 / Her	—	-2.52	—	—	0.02	-0.87
SDSS J163059.32+124725.6 / Her	—	-2.83	—	—	-0.82	< 0.24
SDSS J163104.50+124614.4 / Her	—	-2.53	0.13	—	0.08	-0.47
SDSS J163114.06+124526.6 / Her	—	-2.28	—	-0.24	-0.52	-0.81
SDSS J113255.99-003027.8 / Leo IV – S1	0.26	-2.88	—	—	< -0.02	< -0.98
SDSS J113258.70-003449.9 / Leo IV	-0.14	-2.18	—	—	< -1.42	< -1.38
SDSS J125713.63+341846.9 / CVn II	—	-2.58	—	—	1.32	< -1.28
SDSS J135801.42+125105.0 / Boo II – 7	—	-3.08	—	—	< -1.32	< 0.32
SDSS J135751.18+125136.9 / Boo II – 15	—	-2.98	—	—	< -2.22	< -0.28
SDSS J132844.25+333411.8 / CVn I	—	-2.52	—	—	0.62	-0.14
SDSS J132755.65+333324.5 / CVn I	—	-2.18	—	—	0.58	0.36

The upper part of Fig 2 shows our results for the $[Al/Fe]$ ratios. As for the previous figure, we have added literature data for field stars and dwarf spheroidal galaxy stars. We find a high value of the $[Al/Fe]$ ratio when compared to the halo stars. We did not apply non-LTE corrections in order to make a direct comparison with the halo and DSph stars which have been analyzed under the same assumptions. Sodium seems to share this behavior as shown in the lower part of Fig 2. This high value of $[Na/Fe]$ compared to the ratios in halo stars of the same metallicity has also been found by Koch et al. (2008) in Hercules.

Fig 3 presents the $[Sr/Fe]$ and $[Ba/Fe]$ ratios found for our sample together with literature data for field stars and dwarf spheroidal galaxy stars. The upper graph shows a high value of the $[Sr/Fe]$ ratio for the metal-rich sample of our stars similar to what is found in the halo stars and significantly different from the DSph stars. For the most metal-poor stars of our analysis, the ratio appears to be lower than what found for the bulk of the field halo stars of the same metallicity. For Barium, our results fall also in the range of $[Ba/Fe]$ found for halo stars.

5.1. Bootes II

We have observed two stars in the Galaxy (BooII-7 and BooII-15) and found metallicities $[Fe/H] = -2.98$ dex and -3.08 dex. As the second star has been already observed by Koch & Rich (2014),

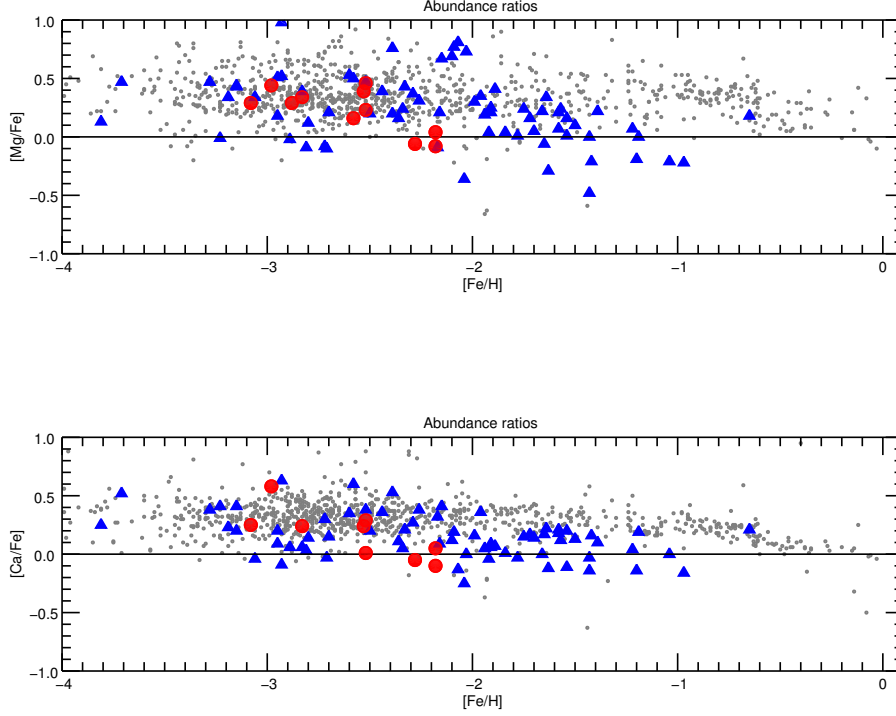


Fig. 1. Alpha elements : Grey circles represent literature data for field stars gathered in Frebel (2010) . Blue triangles are literature data for dwarf spheroidal galaxies. Red circles represent the results for our sample of UfDSph stars.

Table 7. BooII-15 abundance comparison

Ion	This paper	Koch & Rich (2014)
[Fe/H]	-3.08	-2.93
[C/Fe]	-0.10	0.03
[Mg/Fe]	0.44	0.58
[Ca/Fe]	0.58	0.35
[Ba/Fe]	< -0.28	< -0.62

we put the results from both studies in table 7. The results are in general good agreement. The Carbon abundance has been computed by fitting a synthetic spectrum for the CH G band. The $[\alpha/\text{Fe}]$ overabundance and the low $[\text{Ba}/\text{Fe}]$ are characteristic of the galactic halo population. We found a very low upper limit for strontium with a value of $[\text{Sr}/\text{Fe}] \leq -2.22$ dex. We also obtained a comparable low value of strontium for the star Boo-7 with $[\text{Sr}/\text{Fe}] \leq -1.32$ dex. This low value of strontium with respect to what is found in the halo stars of the same metallicity is generally observed in UfDSph galaxies as shown in Fig 3.

5.2. Canes Venatici I

Abundances of Fe, Mg and Ca of a sample of stars belonging to CVnI have been reported by Kirby et al. (2010) using low resolution spectra. Using the same Keck/DEIMOS medium resolution

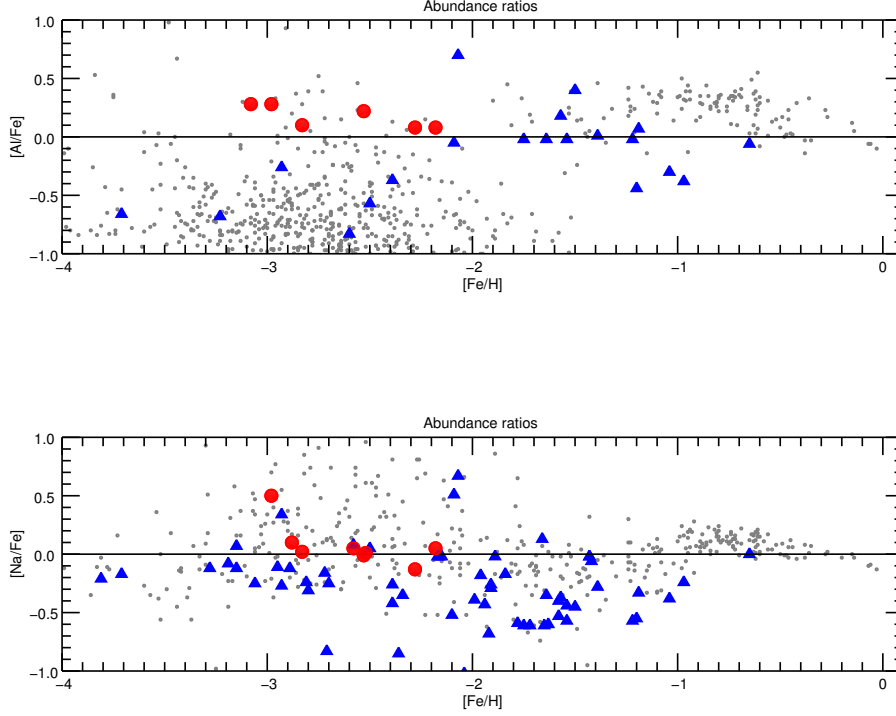


Fig. 2. Al and Na abundance ratios : Grey circles represent literature data for field stars gathered in Frebel (2010). Blue triangles are literature data for dwarf spheroidal galaxies. Red circles represent the results for our sample of UfDSph stars.

spectra obtained by Kirby et al. (2010), Vargas et al. (2013) determine the abundance of Fe, Mg, Ca in stars of this galaxy. On Fig 4, we plotted our results together with the results from Kirby et al. (2010) and Vargas et al. (2013). We have also added the results for a sample of UfDSph galaxies as in Fig 1.

We report for the first time the abundance determination of the neutron capture elements in two stars of this galaxy. We found for both stars a high ratio of $[Sr/Ba]$, +0.22 dex and +0.76 dex respectively. It is interesting to note that these ratios are similar to the one found in the halo stars at the same $[Ba/H]$ abundance as found by François et al. (2007).

5.3. Canes Venatici II

Our results for Canes Venatici II are presented in Fig 5. This is the first Strontium abundance determination for a star in this Galaxy. Our star has a very high $[Sr/Fe]$ values and a low upper limit of $[Ba/Fe]$ which makes it a star with an exceptionally high $[Sr/Ba]$ with a value larger than 2.6 dex.

In Figs 6 and 7 are shown the results from the spectrum synthesis computation superimposed on the data for the line of Barium at 493.4 nm and the line of strontium at 421.5 nm. The blue lines correspond to the abundance ratios we determined whereas the black dotted line represents a spectrum with a solar ratio. The low barium abundance has been confirmed using the lines at 649.7 and 614.1 nm. The high $[Sr/Ba]$ ratio may be explained by invoking different sources for

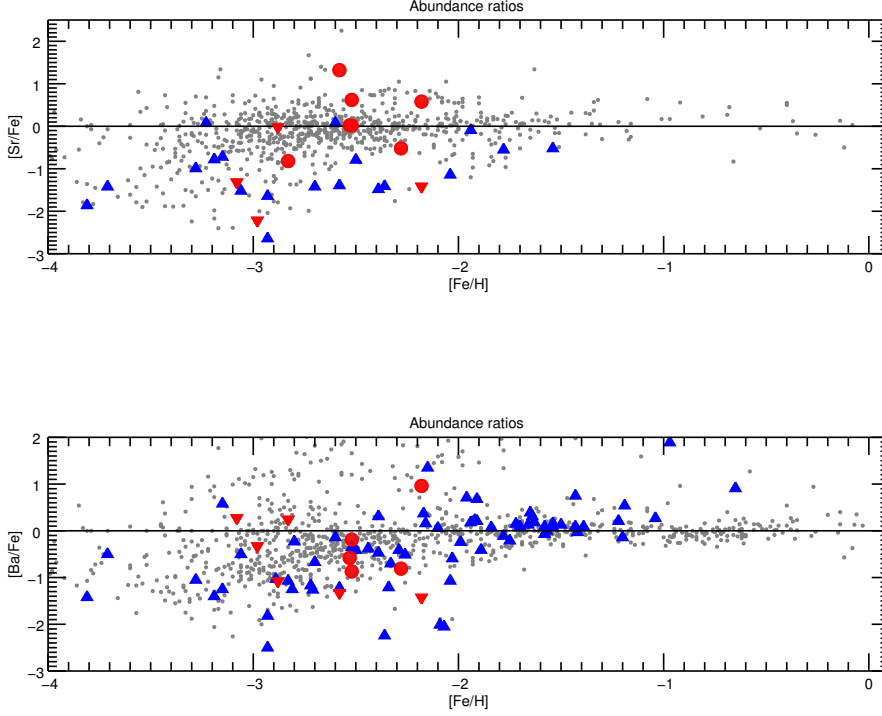


Fig. 3. Neutron capture elements : Grey circles represent literature data for field stars gathered in Frebel (2010). Blue triangles are literature data for dwarf spheroidal galaxies. Red circles represent the results for our sample of UfDSph stars. Red triangles represent upper limits for stars of our sample.

the production of light neutron capture elements versus heavier neutron capture elements. At low metallicity, strontium may be formed by the weak r-process (Wanajo, 2013). The large difference between the two mostly s-process element strontium and barium may come from a peculiar pollution of the cloud which formed the star, the source being possibly a core-collapse supernova as proposed by Wanajo (2013). More recently, Cescutti et al. (2015) have computed detailed models of galactic chemical evolution of our Galaxy. Their computations have shown that the combination of r-process production by neutron star mergers and s-process by spinstars (Pignatari et al., 2008; Frischknecht et al., 2012) is able to reproduce the large range of [Sr/Ba] ratios at low metallicity.

It would be particularly interesting to obtain a high resolution high S/N spectrum of this star in order to detect and measure the abundances of other n-capture elements and compare it with high Sr low metallicity field halo stars.

5.4. Hercules

Koch et al. (2013) studied a sample of 11 red giant stars. They could detect the barium line at 6141.713 Å for three of them. Our results for Hercules are presented as red circles in Fig 8. We have added the results from Koch et al. (2008, 2013) and Adén et al. (2009).

Our sample has metallicities ranging from -2.28 dex to -2.83 dex. Our results show clearly an increase of the $[\alpha/\text{Fe}]$ ratios as the metallicity decreases. It is important to note that this effect has

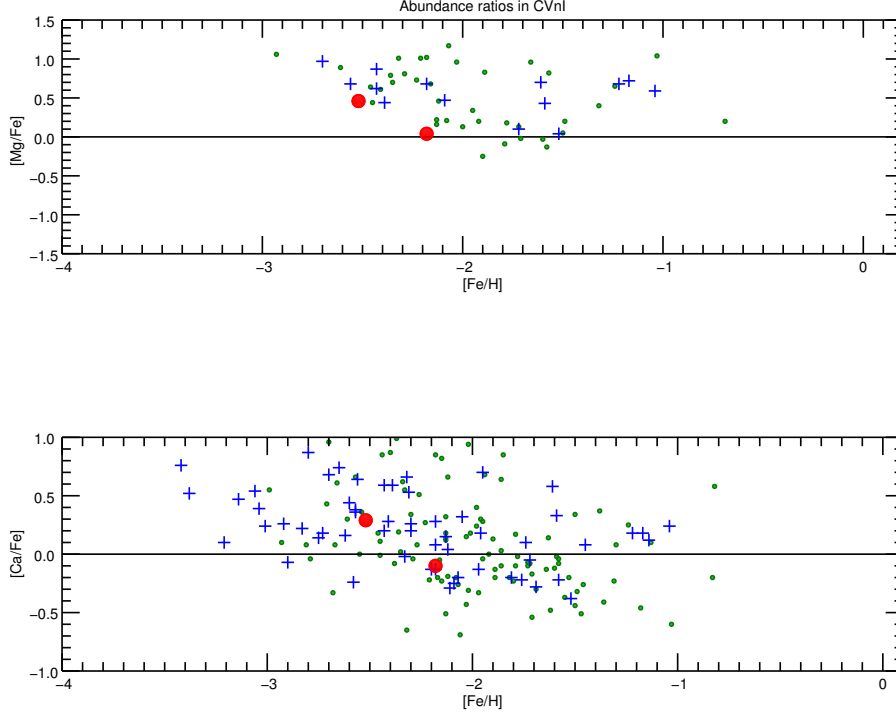


Fig. 4. Abundance results for the CVnI galaxy stars. Red circle represent our two stars. Green symbols are results from Kirby et al. (2010). Blue symbols are results from Vargas et al. (2013)

been already observed by Vargas et al. (2013) not only Hercules but also in other galaxies. This is what is expected with classical models of chemical evolution where the impact of the contribution of type SNIa iron on the abundance ratios $[\alpha/Fe]$ vs metallicity relations is shown as a decrease of this ratio as the metallicity increases. For Her, the solar ratio is reached at a much lower metallicity than the one found for the Milky Way and even the dwarf spheroidal galaxies such as Carina or Sculptor as shown in Vincenzo et al. (2014). Our results for Calcium are in good agreement with the results Adén et al. (2009) although we notice a slightly higher $[Ca/Fe]$ ratio than the one found by Koch et al. (2008, 2013).

In Fig 9 and 10, we show the spectrum synthesis of a barium line with two assumptions for the $[Ba/Fe]$ ratio. The high efficiency of X-Shooter allowed to make a clear detection of the barium line compared to previous studies where only upper limits could be derived.

For barium, the combination of our results with the barium detections from Koch et al. (2008, 2013) seem to indicate an increase of the $[Ba/Fe]$ ratio as the metallicity increases in line with what is found in our Galaxy.

However, this should be taken with caution when we add their Ba upper limits as it would rather reveal a large scatter.

5.5. Leo IV

We observed two stars in Leo IV, one of them has been already studied by Simon et al. (2010). In Table 8, we can compare the results from both studies. The results are in good agreement. The

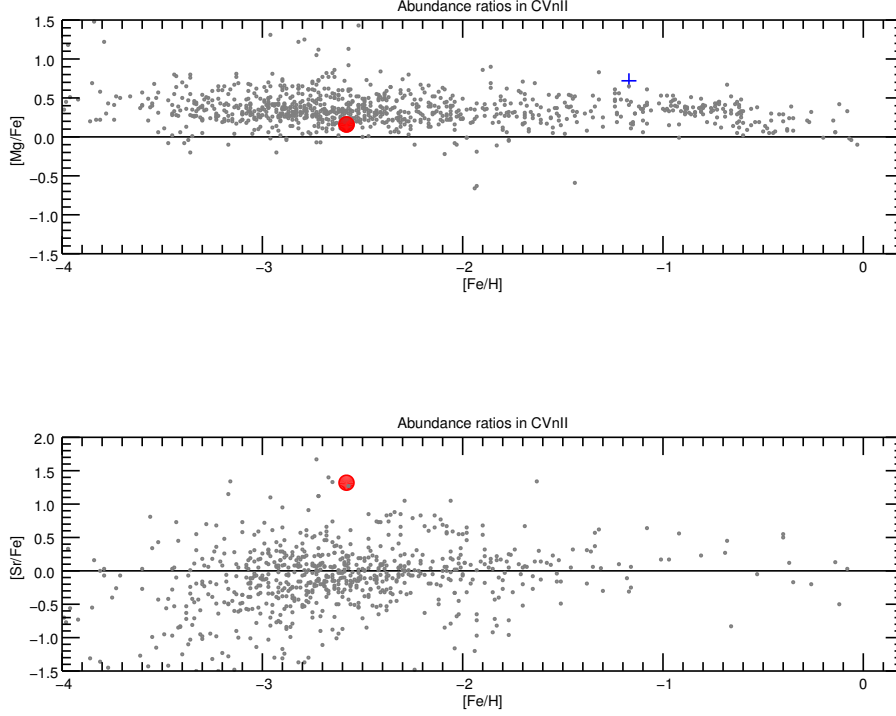


Fig. 5. Abundance results for the CVnII galaxy stars. Red circles represent the abundance results for our stars.

Table 8. Leo IV - S1 abundance ratio comparison

Ion	This paper	Simon et al. (2010)
[Fe/H]	-2.88	-3.20
[Na/Fe]	0.10	0.01
[Mg/Fe]	0.44	0.32
[Ti/Fe]	0.26	0.38
[Sr/Fe]	< -0.02	-1.02
[Ba/Fe]	< -0.98	-1.45

high resolution spectrum used by Simon et al. (2010) allowed to derive the abundance of Ba and Sr. For our second star, we found a higher metallicity with $[Fe/H] = -2.18$ dex, $[Mg/Fe] = -0.06$ dex and $[Ca/Fe] = -0.05$ dex in good agreement with the theoretical predictions from the galactic chemical evolution models of Vincenzo et al. (2014)

5.6. Do fossil galaxies have peculiar abundances ?

Among the fives galaxies studied in this paper, two (Her and Leo IV) have probably formed the bulk of their stars before reionization (Weisz et al. , 2014) It would be therefore be particularly interesting to check whether the abundance ratios reveal any systematic difference between these "fossil" galaxies and the rest of the sample. We have added the results from BooI (Gilmore et al. , 2013) as a member of the galaxy group with an extended star formation history.

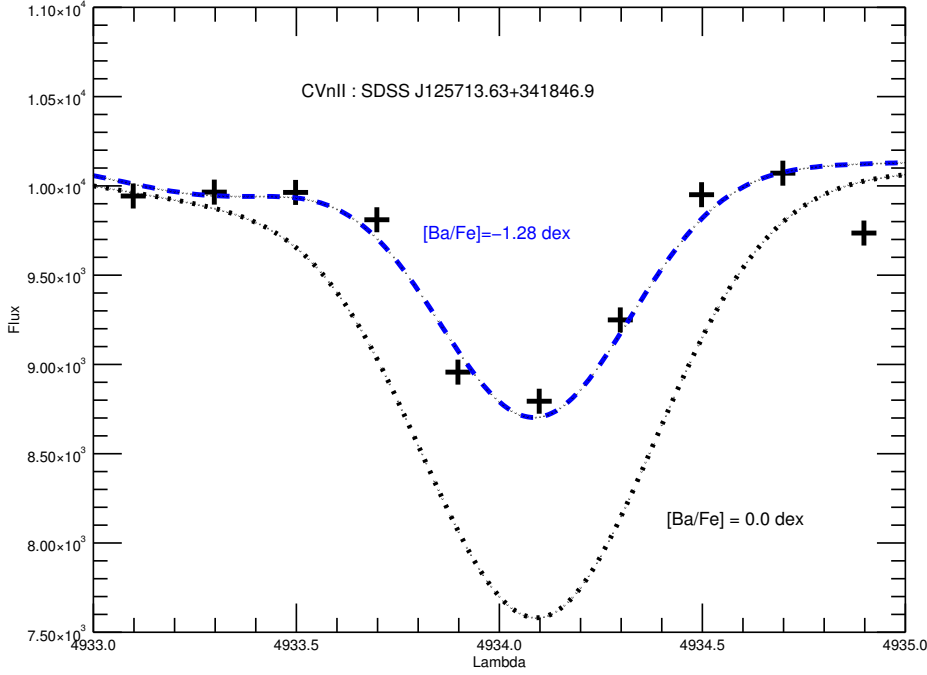


Fig. 6. Comparison of the observed spectrum represented by pluses and synthetic spectra with different barium abundances.

In Fig 11 , we plotted our results and literature data for UfDSph with red symbols for the fossil galaxies and blue symbols for the other galaxies. We also added as reference literature data for the field halo stars as small grey circles. An inspection of the figure seems to indicate the "fossil" galaxies have a lower $[Ca/Fe]$ than the other galaxies and that $[Mg/Fe]$ is also somewhat lower. In Fig 12, we made similar plots for the neutron capture elements Sr and Ba. Again, the "fossil" galaxies seem to have a lower $[Sr/Fe]$ and $[Ba/Fe]$ than the other galaxies. Only the high $[Sr/Fe]$ found in the CVnII star departs from this trend. This result has to be taken with caution as it relies on a small number of stars. Further studies based on a larger sample of galaxies would be necessary to confirm the reality of this effect.

On the assumption the "fossil" group of galaxies have indeed produced the bulk of their stars before reionization, our results, combined with the literature data, suggest that fossil galaxies have lower $[X/Fe]$ ratios at any given metallicity, than the galaxies that have **not** experienced a discontinuity in their SFR (quenching).

The star formation history of quenched galaxies is affected by an episode when the formation of stars is stopped. In terms of galactic chemical evolution, this can be translated by a period where the intermediate mass stars continue their evolution while no stars are formed. These stars are responsible for the enrichment in *s* - *process* elements, such as Sr and Ba.

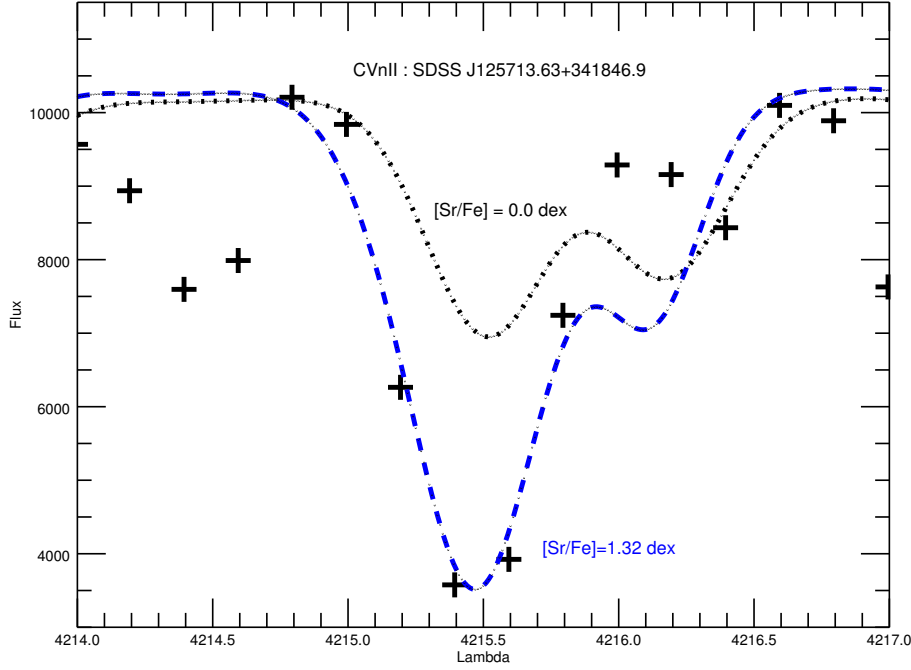


Fig. 7. Comparison of the observed spectrum represented by pluses and synthetic spectra with different strontium abundances.

6. Conclusions

We have reported abundance ratios in a sample of 11 stars belonging to 5 different UfDSphs based on X-Shooter spectra obtained at the VLT. This study demonstrates that X-Shooter is a very powerful instrument to determine the detailed chemical composition of metal-poor stars in UfDSph. With the present analysis based on only a couple of nights of telescope time, we could obtain some interesting results. We can therefore foresee further studies of the detailed chemical evolution of many galaxies of the local group using 10 meter class telescopes and medium resolution spectroscopy at the level of $R \simeq 8\,000$ and higher. From the comparative analysis of the abundances ratios found in these different systems, we can not only study the star formation histories of these galaxies as entities but we can also check for the universality of the nucleosynthesis of the elements. In particular, UfDSph (low mass galaxies) are ideal to study the existence and the frequency of rare events like neutron stars mergers and their impact on nucleosynthesis and galactic chemical evolution.

Considering all the stars as representative of the same population of low mass galaxies, we found that the $[\alpha/\text{Fe}]$ ratios vs $[\text{Fe}/\text{H}]$ decreases as the metallicity of the star increases in a way similar to what is found for the population of stars belonging to dwarf spheroidal galaxies. The main difference is that the a solar $[\alpha/\text{Fe}]$ is reached at a much lower metallicity for the UfDSph than for the dwarf spheroidal galaxies. $[\text{Al}/\text{Fe}]$ and $[\text{Na}/\text{Fe}]$ seem to be give higher values compared to the stars with the same metallicity observed in the halo or in dwarf spheroidal galaxies.

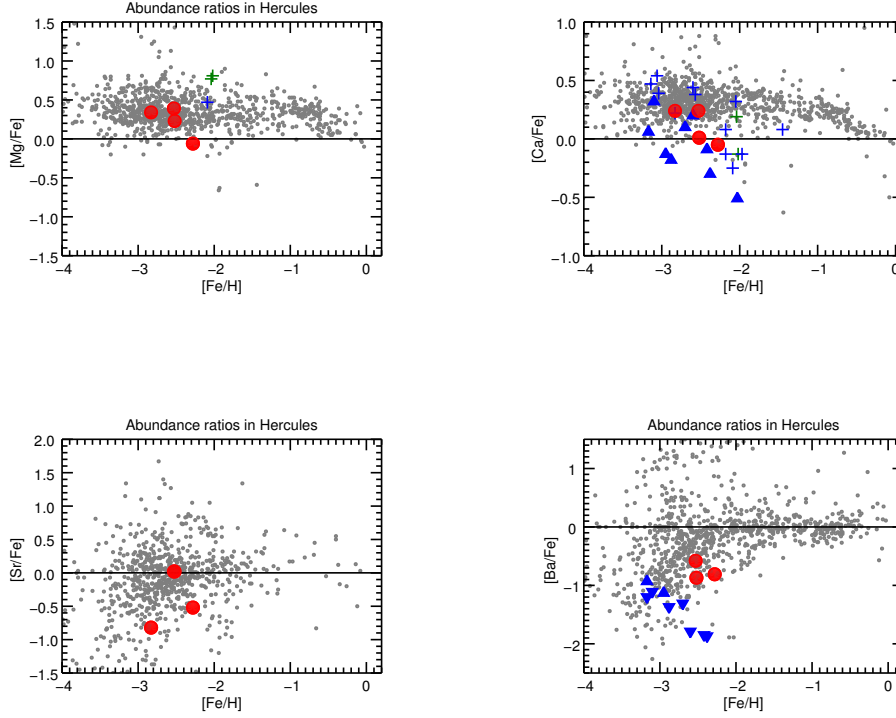


Fig. 8. Our results for Hercules are presented as red circles. We have added the results from Koch et al. (2008, 2013) as blue triangles (triangles pointing down are upper limits) and Adén et al. (2009) as blue pluses. Grey dots are literature data for the field halo stars gathered in Frebel (2010).

We report for the first time the abundance of strontium in CVnI. The star we analyzed in this galaxy has a very high $[\text{Sr}/\text{Fe}]$ and a very low upper limit of barium which makes it a star with an exceptionally high $[\text{Sr}/\text{Ba}]$ ratio.

Based on our results, we suggest that fossil galaxies, that have formed the bulk of their stars before reionization have lower $[X/\text{Fe}]$ ratios than galaxies, of the same metallicity, that have experienced a quenching of their star formation rate.

Acknowledgements. We would like to thank E. Kirby for sending in electronic format the data for the individual stars he studied in his 2008 paper. PF thanks the European Southern Observatory for his support. PF and PB acknowledge support from the Programme National de Physique Stellaire (PNPS) of the Institut National de Sciences de l’Univers of CNRS. LM acknowledges support from ‘Proyecto interno’ of the Universidad Andrés Bello. CMB acknowledges support from FONDECYT regular project 1150060. This research has made use of NASA’s Astrophysics Data System, and of the VizieR catalogue access tool, CDS, Strasbourg, France

References

- Adén, D., Feltzing, S., Koch, A., Wilkinson, M. I., Grebel, E. K., Lundstrom, I., Gilmore, G. F., Zucker, D. B., Belokurov, V., Evans, N. W., Faria, D. 2009 *A&A*, 525, 153
- Adén, D., Eriksson, K., Feltzing, S., Grebel, E. K., Koch, A., Wilkinson, M. I. 2011, *A&A*, 525, 153
- Allen, D., Ryan, S.G., Rossi, S., Beers, T., Tsangarides, S.A. 2012, *A&A* 548, 34
- Alonso, A., Arribas, S., & Martínez-Roger, C. 1999, *A&AS*, 140, 261
- Alvarez, R., & Plez, B. 1998, *A&A*, 330, 1109
- Asplund, M., Gustafsson, B., Kiselman, D., & Eriksson, K. 1997, *A&A*, 318, 521

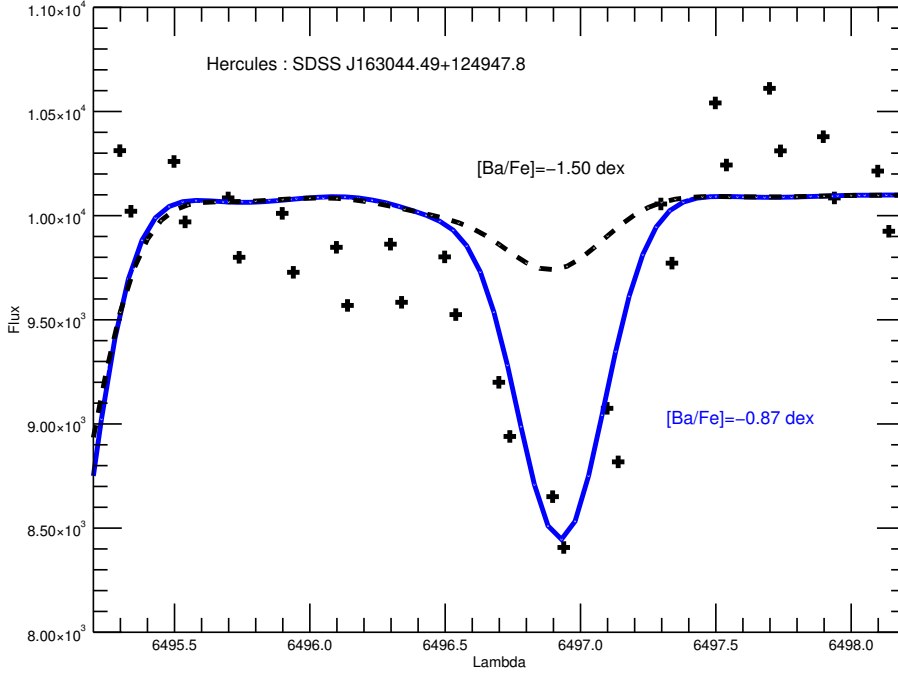


Fig. 9. Comparison of the observed spectrum represented by pluses and synthetic spectra. The dashed black lines is computed for a barium abundance $[Ba/Fe] = -1.50$ dex corresponding to the 3σ upper limit of Koch et al. (2013). The higher quality of the X-Shooter spectra permits the detection of the barium line. The blue line is computed with a barium value $[Ba/Fe] = -0.87$ dex corresponding to our result.

Asplund, M., Grevesse, N., Sauval, A. J., Scott, P. ARA&A47, 481

Belokurov, V., Zucker, D. B., Evans, N. W., Kleyna, J. T., Koposov, S., Hodgkin, S. T., Irwin, M. J., Gilmore, G., Wilkinson, M. I., Fellhauer, M., Bramich, D. M., Hewett, P. C., Vidrih, S., De Jong, J. T. a., Smith, J. a., Rix, H. -W., Bell, E. F., Wyse, R. F. G., Newberg, H. J., Mayeur, P. a., Yanny, B., Rockosi, C. M., Gnedin, O. Y., Schneider, D. P., Beers, T. C., Barentine, J. C., Brewington, H., Brinkmann, J., Harvanek, M., Kleinman, S. J., Krzesinski, J., Long, D., Nitta, A., Snedden, S. a. 2006, ApJ, 654, 906

Brown, Thomas M., Tumlinson, Jason, Geha, Marla, Simon, Joshua D., 2014 ApJ, 796, 91

Bullock, J. S., Kravtsov, A. V., Weinberg, D. H. 2000, ApJ, 539, 517

Caffau, E., Bonifacio, P., François, P. et al. 2011 A&A, 542, 4

Caffau, E., Ludwig, H.-G., Steffen, M., Freytag, B., Bonifacio, P. 2011 Solar Phys 268, 255

Cescutti, G., Romano, D., Matteucci, F., Chiappini, C., Hirshi, R. 2015, A&A577, 139

Coleman, M. G., de Jong, J. T. , Martin, N. F. , 2007 ApJ, 668, 43

D’Odorico, S., Dekker, H., Mazzoleni, R. et al. 2006 SPIE 6269, 33

Edvardsson, B., Andersen, J., Gustafsson, B., et al. 1993, A&A, 275, 101

François, P., Depagne, E., Hill, V., Spite, M. et al. 2007 A&A, 476, 935

Frebel, A 2010, Astronomische Nachrichten, 331, 474

Frischknecht, U., Hirschi, R., Thielemann, F.-K. 2012, A&A, 538, L2

Gilmore, G., Norris, J. E., Monaco, L. , Yong, D., Wyse, R. F. G. Geisler, D. ApJ, 763, 61

Goldoni, P., Royer, F., François, P., Horrobin, M., Blanc, G., Vernet, J., Modigliani, A., Larsen, J. 2006 SPIE 6269, 2

Gratton, R.G., Sneden, C. 1994 /aap 287, 927

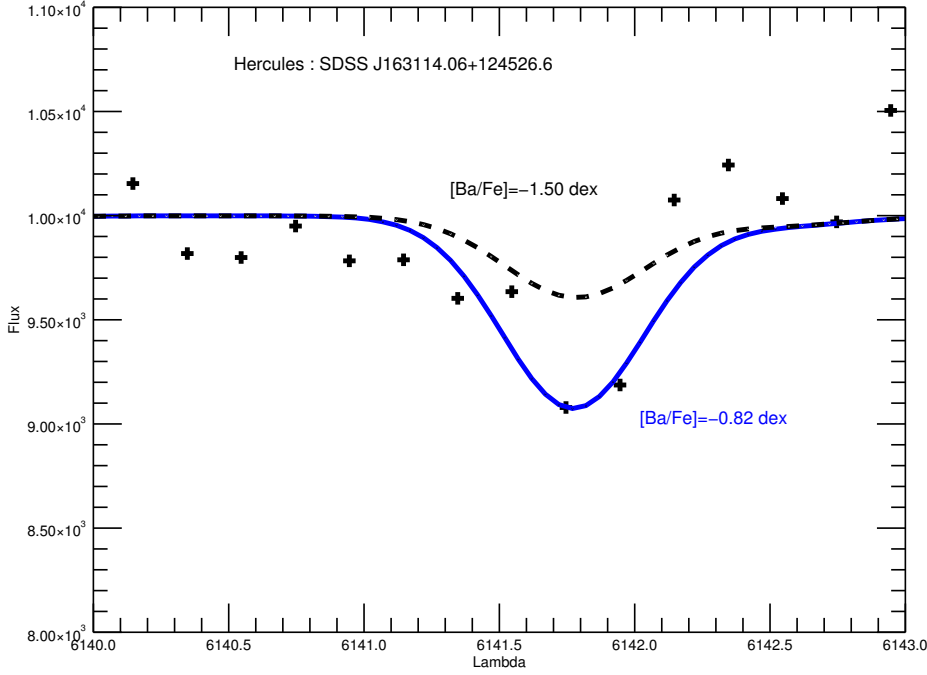


Fig. 10. Comparison of the observed spectrum represented by pluses and synthetic spectra. The dashed black lines is computed for a barium abundance $[Ba/Fe] = -1.50$ dex corresponding to the 3σ upper limit of Koch et al. (2013). The higher quality of the X-Shooter spectra permits the detection of the barium line. The blue line is computed with a barium value $[Ba/Fe] = -0.81$ dex corresponding to our result.

- Greco, C., Dall’Ora, M., Clementini, G., Ripepi, V., Di Fabrizio, L., Kinemuchi, K., Marconi, M., Musella, I., Smith, H. A., Rodgers, C. T., Kuehn, C., Beers, T. C., Catelan, M., Pritzl, B. J. 2008, *ApJ* 675, 73
- Grevesse, N. & Sauval, A. J. 2000, *Origin of Elements in the Solar System*, ed. O. Manuel, 261
- Gustafsson, B., Bell, R. A., Eriksson, K., & Nordlund, A. 1975, *A&A*, 42, 407
- Gustafsson, B., Edvardsson, B., Eriksson, K., et al. 2003, in *Stellar Atmosphere Modeling*, ed. I. Hubeny, D. Mihalas, & K. Werner, ASP Conf. Ser., 288, 331
- Gustafsson, B., Edvardsson, B., Eriksson, K., Jorgensen, U. G., Nordlund, A., Plez, B. 2008, *A&A*, 486, 951
- Hill, V., Plez, B., Cayrel, R. et al. 2002, *A&A*, 387, 560
- Jordi, K., Grebel, E. K., Ammon, K. *A&A*, 460, 339
- Kelson, D. 2003 *PASP*, 115, 688
- Kirby, E. N., Guhathakurta, P., Simon, J. D., Geha, M. C., Rockosi, C. M., Sneden, C., Cohen, J. G., Sohn, S. T., Majewski, S. R., Siegel, M. 2010 *ApJS*, 191, 352
- Kirby, E. N., Lanfranchi, G. A., Simon, J. D., Cohen, J. G., Guhathakurta, P. 2011 *ApJ*, 727, 78
- Kirby, E. N., Simon, J. D., Geha, M., Guhathakurta, P. and Frebel A. 2008 *ApJ*, 685, L43
- Koch, A., McWilliam, A., Grebel, E. K., Zucker, D. B., Belokurov, V. 2008, *ApJ*, 688, L13
- Koch, Andreas, Wilkinson, Mark I., Kleyna, Jan T., Irwin, Mike, Zucker, Daniel B., Belokurov, Vasily, Gilmore, Gerard F., Fellhauer, Michael, Evans, N. Wyn 2009, *ApJ*, 690, 453
- Koch, A., Feltzing, S., Adén, D., Matteucci, F. 2013, *A&A*, 554, 5
- Koch, Andreas, Rich, R. Michael 2014, *ApJ*, 794, 89
- Kuehn, C., Kinemuchi, K., Ripepi, V., Clementini, G., Dall’Ora, M., Di Fabrizio, L., Rodgers, C. T., Greco, C., Marconi, M., Musella, I., Smith, H. A., Catelan, M., Beers, T.C., Pritzl, B. 2008 *ApJ* 674, 81

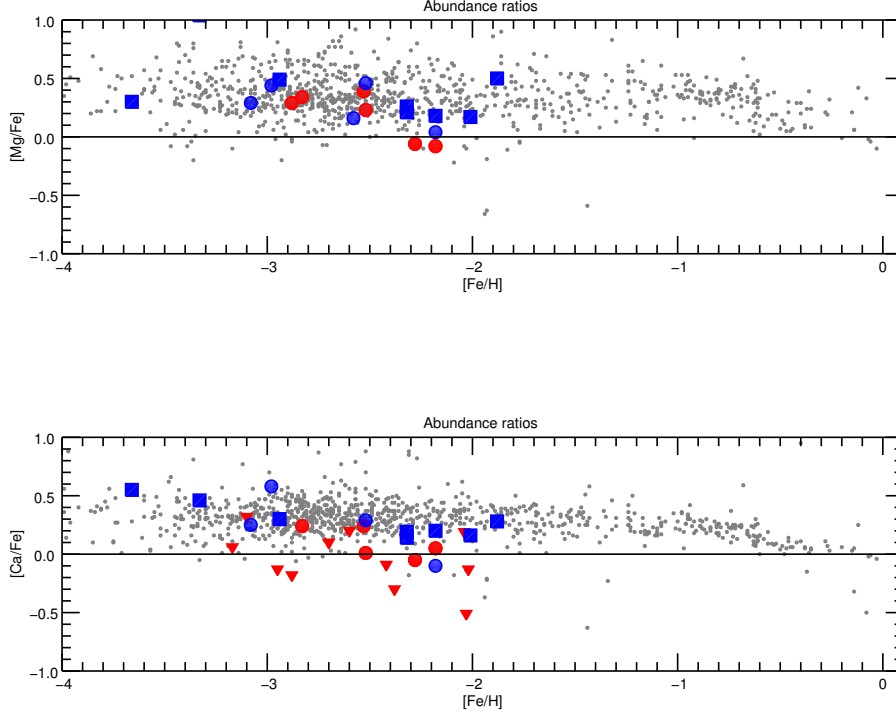


Fig. 11. Our results for Hercules and LeoIV are presented as red circle . We have added the results from Koch et al. (2008, 2013) and Adén et al. (2009) as red triangles (triangles pointing down are upper limits) . Blue circles are our results for the remaining galaxies. Blue squares are literature data for BooI. Grey dots are literature data for the field halo stars gathered in Frebel (2010).

- Lemasle, B., François, P., Piersimoni, A., Pedicelli, S., Bono, G., Laney, C. D., Primas, F., Romaniello, M. 2008 A&A490, 613
- Lodders, L., Palme, H., Gail, H-P, LanB 4, 44 Abundances of the elements in the Solar System. Trumper, J.E. (ed.), Landolt-Bornstein (Springer-Verlag, Berlin)
- Ludwig, H.-G., Bonifacio, P., Caffau, E., Behara, N. T., Gonzalez Hernandez, J. I., Sbordone, L. 2008 Phys. Scr, 133
- McWilliam, A., Preston, G. 1995 AJ, 106,2757
- Martin, Nicolas F. Coleman, M. G., De Jong, J. T. a., Rix, H-W., Bell, E. F., Sand, D. J., Hill, J. M., Thompson, D., Burwitz, V., Giallongo, E., Ragazzoni, R., Diolaiti, E., Gasparo, F., Grazian, A., Pedichini, F., Bechtold, J. 2008 ApJ, 672, L13
- Moore, B., Ghigna, S., Governato, F. et al, ApJ, 524, L19
- Moretti, M. I., Dall’Ora, M., Ripepi, V., Clementini, G., Di Fabrizio, L., Smith, H., De Lee, N., Kuehn, C., Catelan, M., Marconi, M., Musella, I., Beers, T., Kinemuchi, K. 2009 ApJ, 699, 125
- Musella, I., Ripepi, V., Marconi, M., Clementini, G., Dall’Ora, M., Scowcroft, V., Moretti, M. I., Di Fabrizio, L., Greco, C., Coppola, G., Bersier, D., Catelan, M., Grado, A., Limatola, L., Smith, H. A., Kinemuchi, K. 2012, ApJ756, 121
- Okamoto, S., Arimoto, N., Yamada, Y., Onodera, M. 2012, ApJ, 744, 96
- Pignatari, M., Gallino, R., Meynet, G., Hirschi, R., Herwig, F., Wiescher, M. 2008, A&A, 687, L95
- Plez, B., Brett, J. M., & Nordlund, A. 1992, A&A, 256, 551
- Ramírez, Iván, Meléndez, Jorge 2005 ApJ, 626, 465
- Ricotti, M. & Gnedin, N. Y. 2005 ApJ, 629, 259
- Roderick , T.A., Jerjen H., Mackey A. D. , Da Costa G. arXiv : 1503.03896
- Schlegel, D. J., Finkbeiner, D. P., Davis, M. 1998 ApJ, 500, 525
- Simon, J. D., Geha, M. 2007, ApJ, 670, 313
- Simon, J. D., Frebel, A., McWilliam, A., Kirby, E. N., Thompson, I. B. 2010, ApJ, 716, 446

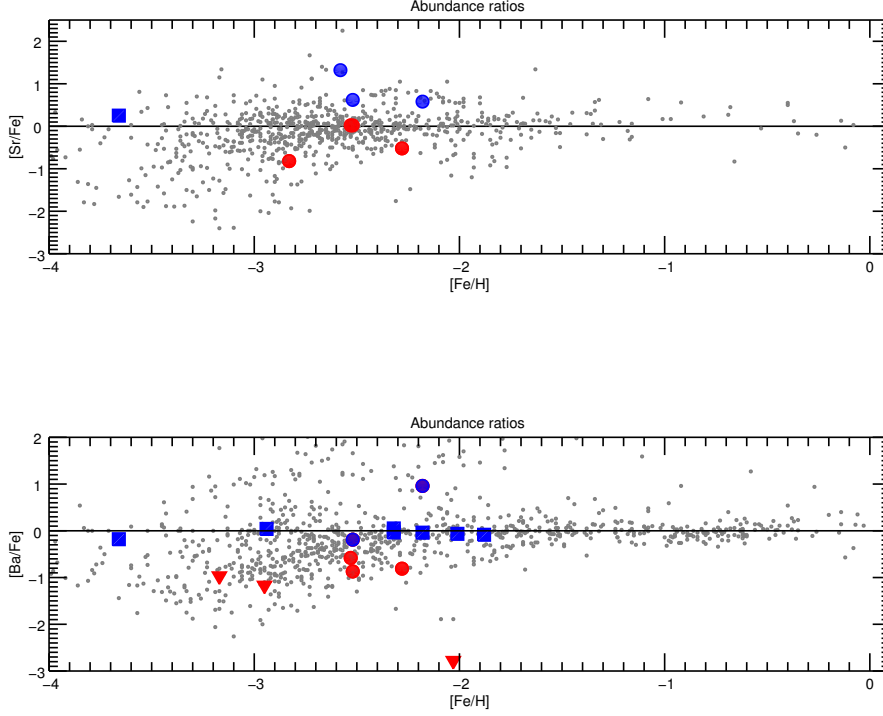


Fig. 12. Our results for Hercules and LeoIV are presented as red circle . We have added the results from Koch et al. (2008, 2013) and Adén et al. (2009) as red triangles (triangles pointing down are upper limits) . Blue circles are our results for the remaining galaxies. Blue squares are literature data for BooI. Grey dots are literature data for the field halo stars gathered in Frebel (2010).

- Ural, Ugur, Wilkinson, M. I., Koch, A., Gilmore, G., Beers, T. C., Belokurov, V., Evans, N. W., Grebel, E. K., Vidrih, S., Zucker, D. B. 2010 MNRAS402,1357
- Van Dokkum, P. 2001 PASP, 562, 35
- Vargas, L. C., Geha, M., Kirby, E. N., Simon, J. D. 2013, ApJ, 767, 134
- Vernet, J., Dekker, H., D’Odorico, S 2011 A&A, 536, 105
- Vincenzo, F., Matteucci, F., Vattakunnel, S., Lanfranchi, G. A. 2014 MNRAS 441, 2815
- Wanajo, S., 2013 , ApJ770, L12
- Weisz, Daniel R., Dolphin, Andrew E., Skillman, Evan D., Holtzman, Jon, Gilbert, Karoline M., Dalcanton, Julianne J., Williams, Benjamin F. 2014, ApJ, 789, 148
- Weisz, D. R., Dolphin, A. E., Skillman, E. D., Holtzman, J., Gilbert, K. M., Dalcanton, J. J., Williams, B. F. ApJ, 804,136
- Walsh, S.M., Jerjen, H., Willman, B. 2007, ApJ, 662, L83
- Walsh, S., Jerjen, H., Willman, B. 2008 Galaxies in the Local Volume, Astrophysics and Space Science Proceedings, ISBN 978-1-4020-6932-1. Springer Netherlands, 2008, p. 191
- Webster, D., Bland-Hawthorn, J., Sutherland, . 2015 ApJ799, 21
- Zucker, D B, Belokurov, V, Evans, N W, Wilkinson, M I, Irwin, M J, Sivarani, T, Hodgkin, S, Bramich, D M, Irwin, J M, Gilmore, G, Willman, B, Vidrih, S, Fellhauer, M, Hewett, P C, Beers, T C, Bell, E F, Grebel, E K, Schneider, D P, Newberg, H J, Wyse, R F G, Rockosi, C M, Yanny, B, Lupton, R 2006, ApJ, 643, 103